Carson, B., Westbrook, G.K., Musgrave, R.J., and Suess, E. (Eds.), 1995
Proceedings of the Ocean Drilling Program, Scientific Results, Vol. 146 (Pt. 1)

10. RELATION BETWEEN PORE FLUID CHEMISTRY AND GAS HYDRATES ASSOCIATED WITH BOTTOM-SIMULATING REFLECTORS AT THE CASCADIA MARGIN, SITES 889 AND 892[1]

Miriam Kastner,[2] Keith A. Kvenvolden,[3] Michael J. Whiticar,[4] Angelo Camerlenghi,[5] and Thomas D. Lorenson[3]

ABSTRACT

Prominent seismic bottom-simulating reflectors (BSRs) were penetrated at two sites on the Cascadia Margin, off Vancouver Island (Site 889, at 224 mbsf) and off Oregon (Site 892, at 74 mbsf). Although solid gas hydrate was not recovered at the depth of either of these prominent BSRs, the –1.4°C temperature measured in a core ~8 m above the BSR depth at Site 889, and the observed coincidence of very low pore fluid Cl and very high headspace methane concentrations at the depth of both BSRs, together with an increase in seismic velocities, strongly imply the presence of gas hydrate in situ with methane as the dominant gas within the hydrate cages. Pore-space occupancy by hydrate of a minimum of 15% and ~10% at Sites 889 and 892, respectively, is inferred from geochemical and geophysical evidence. Assuming, however, bottom-water Cl concentration, the maximum Cl dilutions observed, 36% at Site 889 and 15% at Site 892, correspond to pore-space hydrate occupancies of 39% and 16%, respectively. Mixing with a diffusing, or upward-migrating, low-Cl fluid from a deeper source at Sites 889 and 892 accounts for the difference between the two estimates. As gas hydrate was not recovered, it is suggested that finely disseminated hydrate prevails at these sites. Thus, the high amplitudes of these BSRs are not solely related to gas hydrate content, but also to the presence and concentration of free gas below the BSR. The persistence of the zone of maximum Cl dilution below the BSR depth (Site 889) probably reflects a rather recent, interglacial, upward migration of the base of the hydrate stability field.

At both sites the measured in situ borehole temperatures at the depth of the seismic BSRs are lower by approximately 2°C than the calculated temperatures for the base of a pure H_2O–pure CH_4 hydrate stability field at the corresponding pressures. Addition of gases such as ethane, CO_2, or H_2S further increases the hydrate stability temperature at corresponding pressures. The measured temperatures, however, are within the uncertainties of the base of the stability field of a seawater-CH_4 hydrate. This observation has important implications for using seismic BSRs for mapping heat flow.

Solid gas hydrate was recovered only at Site 892 between 2 and 19 mbsf, but this gas hydrate was not associated with the BSR, which occurs at a depth of 74 mbsf. This is a mixed hydrate that contains both CH_4 and up to 10% H_2S, with minor amounts of ethane and some CO_2.

INTRODUCTION

Gas hydrates are crystalline substances of an expanded solid-water lattice with cages containing guest gaseous hydrocarbon molecules bonded by Van der Waals forces, which occur under conditions of low to moderate pressures and low temperatures. Methane hydrate is the most common natural gas hydrate in the marine environment. In the modern ocean, methane-hydrate may form in sediments where water depths exceed 300 to 500 m to a subsurface depth of up to about 1100 meters below seafloor (mbsf) (Kvenvolden and McMenamin, 1980).

In addition to temperature and pressure, the stability of gas hydrate depends on the amount and composition of the guest gas(es) and on the chemistry of the pore fluid, especially its salinity. Favorable temperature-pressure conditions for the formation of hydrocarbon gas hydrates exist at the seafloor at all holes drilled during Leg 146 (e.g., Kvenvolden and McMenamin, 1980; Sloan, 1990; Englezos and Bishnoi, 1988, and references therein). Leg 146 was only the second Ocean Drilling Program (ODP) leg with sites purposely located to penetrate bottom-simulating seismic reflectors (BSRs). BSRs appear on marine seismic records and result from the acoustic impedance contrast between gas hydrate-bearing sediment lying above sediment devoid of gas hydrate and/or containing free gas. During ODP Leg 141, at Site 859 in the vicinity of the Chile Triple Junction, the sediment section that included the BSR was logged for the first time. On the basis of the geochemical and geophysical evidence, Bangs et al. (1993) concluded that there is insufficient hydrate above the BSR to produce the large impedance difference at the interface between the hydrate-bearing and hydrate-free sediments. The presence of a very small amount of free gas beneath the BSR provides a reasonable explanation for the existence of the seismic reflection.

A major objective of Leg 146 was to investigate the nature of prominent BSRs, and to determine their relationship to the presence and amount of gas hydrate and/or free gas at the Cascadia margin. A major objective of this paper is to determine the relationship between pore fluid chemistry and gas hydrate associated with these prominent BSRs. Site 889 off Vancouver Island is dominated by diffusive fluid flow, whereas Site 892 offshore from Oregon is dominated by confined-fluid flow (Kastner et al., this volume; Foucher, this volume). Adjacent to Site 892, at the hydrologically active fault that was intersected by drilling, the BSR is displaced upward toward the seafloor as a consequence of warming from the rising fluids (Moore et al., 1990; Davis et al., this volume). The locations of these sites are shown in Figure 1.

[1]Carson, B., Westbrook, G.K., Musgrave, R.J., and Suess, E. (Eds.), 1995. *Proc. ODP, Sci. Results*, 146 (Pt. 1): College Station, TX (Ocean Drilling Program).

[2]Scripps Institution of Oceanography, University of California, San Diego, La Jolla, CA 92093, U.S.A.

[3]U.S. Geological Survey, 345 Middlefield Road, MS-999, Menlo Park, CA 94025, U.S.A.

[4]School for Earth and Ocean Sciences, University of Victoria, Victoria, British Columbia V8W 2Y2, Canada.

[5]Osservatorio Geofisico Sperimentale, Dipartimento di Geofisica della Litosfera, I-34016 Trieste Opicina, Italy.

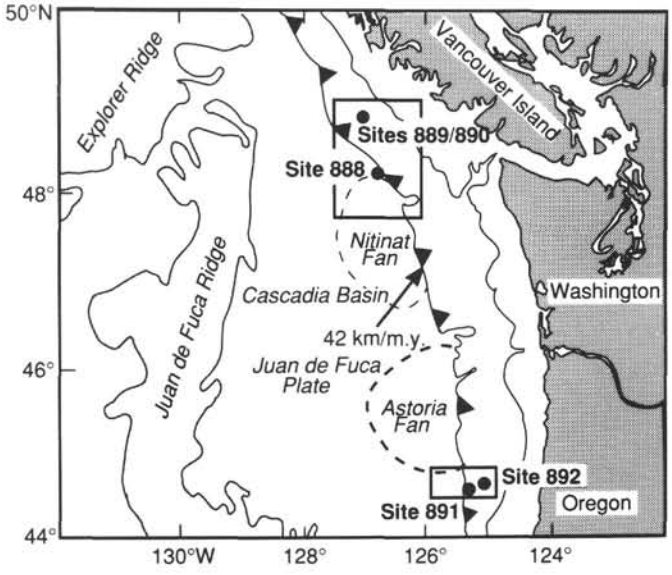

Figure 1. Location of Cascadia Margin sites drilled during ODP Leg 146 (from Westbrook, Carson, Musgrave, et al., 1994).

The prominent seismic BSR at Site 889 is located at ~224 mbsf (from seismic reflector and downhole logging data). Although solid gas hydrate was not recovered at this site, its presence is inferred from geophysical and geochemical measurements and from sedimentological observations (Westbrook, Carson, Musgrave, et al., 1994). Vertical seismic profile (VSP) data at Site 889 show a rise in velocity above the BSR (MacKay et al., 1994). Assuming a bottom-water Cl concentration, a Cl dilution of 36%, corresponding to a 39% methane hydrate occupancy, was determined for the depth just above the BSR. Also, a temperature of –1.4°C was measured in a section of a core at ~217 mbsf, indicating in situ gas hydrate dissociation. However, this temperature measurement suggests that only ~3% of the pore space was filled with gas hydrate, which dissociated during the drilling and core recovery operations. This amount of hydrate is insufficient to produce the impedance difference observed at this BSR, as originally suggested by Hyndman et al. (1992) and Hyndman and Davis (1992). Furthermore, the rather frequent occurrence of unusually wet, "soupy," sediment intervals predominantly in cores within the modern methane hydrate stability field, relative to the section beneath the BSR, suggests that the wetness of these "soupy" intervals reflects dissociation of disseminated gas hydrate upon core recovery. All these indications of gas hydrate, when combined with the observation of lower than seawater VSP velocities immediately below the BSR, suggest at least a moderate amount of gas hydrate above the BSR and a small amount of free gas below it (Westbrook, Carson, Musgrave, et al., 1994; MacKay et al., 1994).

The measured in situ temperature at the Site 889 seismic BSR is lower by approximately 2°C than the calculated temperature for the base of the pure H_2O–pure CH_4 hydrate stability field at the corresponding pressure (Katz et al., 1959; see compilation by Sloan, 1990). If no uncertainties in the temperature and depth of BSR estimates are assumed, it is also lower, by almost 1°C, than the calculated temperature for the base of the seawater-CH_4 hydrate stability field (Dholabhai et al., 1991; Dickens and Quinby-Hunt, 1994).

Neither the sonic-log nor the VSP data show distinct anomalous velocities above the prominent seismic BSR located in Hole 892C at ~74 mbsf, suggesting the presence of only small amounts of gas hydrate, if any (MacKay et al., this volume). No solid gas hydrate was recovered at or in the vicinity of the BSR depth. The observed maximum Cl dilution of 15% at the BSR depth, which corresponds to ~16% methane hydrate pore-space occupancy, is sufficient to cause only a small part of the acoustic impedance difference observed across the BSR interface. The VSP velocities, which indicate the presence of free gas beneath the BSR, could be responsible for most of the BSR amplitude (Westbrook, Carson, Musgrave, et al., 1994; MacKay et al., 1994). At this site, "soupy" sediment intervals occur only within the methane hydrate stability field, above the BSR. Despite the different geological setting of Site 892, the disparities between the measured in situ temperature at the seismic BSR and the calculated temperatures for the bases of the pure H_2O–pure CH_4 and the seawater-CH_4 hydrate stability fields, are almost identical to those encountered at Site 889, which are ~2° and ~1°C, respectively.

Although gas hydrate was not recovered in the vicinity of the BSR at Site 892, unexpectedly, gas hydrate samples were recovered in shallow cores between 2 and 19 mbsf at this site. Unlike previous gas hydrate samples recovered from DSDP or ODP cores, which were predominantly methane hydrate, the gas hydrate found at Site 892 contains both methane and up to 10% H_2S.

GEOLOGIC SETTING

Site 889 is located on a gently undulating 15–20 km-wide seafloor mid-slope terrace of the continental margin off Vancouver Island, at 1320 m water depth (Fig. 1). This region is separated from the lower slope by a steep escarpment of about 1 km relief. Stratified upper Quaternary to lower Pleistocene hemipelagic sediments with interbedded turbidite slope deposits cover the underlying deformed accreted Pliocene clayey silts and sands. These accreted sediments are characterized by laterally incoherent seismic reflectors and a well-developed BSR at ~224 mbsf (Hyndman and Spence, 1992). Diagenetic carbonates, although not plentiful, do occur throughout the section. No important thrust faults exist in the vicinity of this drill site. The geothermal gradient measured during Leg 146 was 54°C/km and was linear with depth (Westbrook, Carson, Musgrave, et al., 1994).

Site 892 is located on the western flank of the second ridge, ~16 km east of the thrust front, on accreted sediments of the lower continental slope off Oregon, at 670 m water depth (Fig. 1). These Pliocene terrigenous silty-clay sediments with interlayered sand were deposited in an abyssal plain environment. Beneath the ridge, the sub-bottom seismic reflectors have poor lateral coherence. At this site, in addition to lesser faults, an out-of-sequence, prominent landward-dipping thrust fault was intersected. Its surface trace, located ~0.5 km west of the site, is associated with a massive bioherm and benthic community, indicating that the fault zone is, and has been, an active aquifer (e.g., Kulm et al., 1986; Moore et al., 1990; Carson et al., 1990, 1994, and references therein). Because the section is cut by several faults, physical properties are discontinuous with depth. Little or no increase in consolidation occurs below the BSR depth (~74 mbsf). Diagenetic carbonate nodules, cement, and layers are widespread throughout the section. Seismic reflection data from these sediments are characterized by a distinct BSR, which, west of this locality, is deflected upward at its intersection with the active fault (Moore et al., 1990). Except for two positive temperature excursions of 1.6° and 2.5°C at 67.5 and 87.5 mbsf, respectively, in Hole 892A, the geothermal gradient measured during Leg 146 is 51°C/km and is linear with depth (Graham, Carson, Musgrave, et al., 1994).

NATURE OF THE BSRS AT SITES 889 AND 892

Background

At three previous DSDP and ODP locations, the Blake-Bahama Outer Ridge, Peru Margin, and Nankai Trough, the depth of the BSR, although within the measurement uncertainties of the seawater-methane stability field, correlates well with the inferred base of the stabil-

ity field of a pure H_2O–pure CH_4 gas hydrate (Hyndman et al., 1992). Based on the measured geothermal gradients at Sites 889 and 892, however, a significant difference exists between the depths of the seismically defined position of the BSR and the pure H_2O–pure CH_4 hydrate stability field. At both sites the seismic BSR occurs at a shallower depth, equivalent to ~2°C lower temperature, than the calculated depth of the base of the pure H_2O–pure CH_4 stability field. At Sites 889 and 892 the seismic BSRs are at ~224 (14.8° C) and ~74 (8.5°C) mbsf, respectively (Westbrook, Carson, Musgrave, et al., 1994; MacKay et al., 1994), and the calculated bases of the pure H_2O–pure CH_4 stability field, at the corresponding geothermal gradients of 54°C/km and 51°C/km, are 260 (16.8° ± 0.2°C) and 112 (10.4° ± 0.2°C) mbsf, respectively. An almost identical disparity between these two depths was observed at the ChileTriple Junction, Site 859 (Bangs et al., 1993).

The BSR that underlies most of the Cascadia Margin was postulated to be caused by the presence of considerable amounts of gas hydrate (~50% of pore space occupancy, >5 m thick layer, Hyndman et al., 1992), but none was recovered at either site. The following questions thus arise:

1. Is gas hydrate present at the Cascadia margin?
2. Is the amplitude of the BSR directly related to gas hydrate content?
3. If gas hydrate dissociates prior to core recovery, is the Cl concentration of the pore water a reliable measure for the amount of dissociated gas hydrate?
4. What is the cause of the Pressure–Temperature (P–T) deviation of the base of the gas hydrate stability field away from the pure H_2O–pure CH_4 curve at these sites and at the Chile Triple Junction, or toward this curve at the Blake-Bahama Outer Ridge, offshore from Peru, and at the Nankai Trough?

In order to address these questions, the relevant geophysical, geochemical, and sedimentological observations at each of the sites are summarized in Table 1 and discussed below.

Evidence for the Presence and Content of Gas Hydrate Above the BSR

The geophysical, geochemical, and sedimentological evidence for the presence and content of gas hydrate associated with the BSR at Sites 889 and 892 consists of:

1. Velocity-depth profiles across the BSRs.
2. Temperature of a core measured upon retrieval.
3. Chloride (and other components) concentration-depth profiles across the BSRs.
4. Depth distribution of unusually wet, "soupy" sediment intervals.
5. Gas composition.

Velocity-depth Profiles across the BSRs

At Site 889 above the BSR, from 130 to 224 mbsf, sonic-log and VSP velocities are greater than expected by ≥100 m/s from normal velocity-porosity relations, suggesting the presence of gas hydrate of at least 15% pore space occupancy. The increase in velocity is not associated with low neutron porosity or high density and resistivity, characteristic of diagenetic induration (Serra, 1984). At Site 892, however, sonic-log or VSP velocity increases above the BSR are not very distinct, suggesting the presence of ≤10% gas hydrate. At both sites, just below the BSR, a marked drop in sonic-log and VSP velocities to near that of water velocity was recorded, indicating low concentrations of free gas. The BSR amplitude is apparently related as much to the amount of gas than to the amount of gas hydrate at Sites 889 and 892. For a detailed discussion of the velocity structures and relations to the BSRs at these sites, see Westbrook, Carson, Musgrave, et al. (1994) and MacKay et al. (this volume).

These geophysical observations imply that, at Site 889, ≤10–20% of the pore space is filled with gas hydrate that has dissociated during core recovery operations (MacKay et al., this volume). On the basis of the gas chemistry (Westbrook, Carson, Musgrave, et al., 1994; Whiticar et al., this volume), it is primarily a methane hydrate, possibly including some CO_2 and ethane. The presence of N_2 and O_2, however, strongly suggests that air contamination is responsible for at least some of the CO_2 observed.

The bases of the low-velocity zones immediately below the BSRs were not reached in the downhole logging, but their thicknesses from seismic data are inferred to be ~15 m and ~50 m at Sites 889 and 892, respectively (MacKay et al., 1994). Thus vertical advection of methane is an unlikely source of the high methane concentrations near and at the depth of the BSRs. Two other possible methane sources are lateral advection or in situ dissociation of pre-existing gas hydrate, beneath the present BSR. The geochemical depth profiles acquired on board the *JOIDES Resolution* (Westbrook, Carson, Musgrave, et al., 1994) and shore-based analyses (shown in Figures 2, 3, and 4) do not support lateral fluid advection at the appropriate depth interval at Site 889. However, the Hole 892A data do support lateral fluid advection at the BSR (~68 mbsf), where a 1.6°C temperature anomaly (Westbrook, Carson, Musgrave, et al., 1994), may possibly be sufficient to influence the in situ gas hydrate stability.

Uplift of the seafloor as a result of sedimentation or tectonic elevation, and/or warming of the bottom water following the last glacial maximum would prompt upward movement of the base of the stability field and in situ dissociation of gas hydrate. (A present-day uplift

Table 1. Comparison of data for Sites 889 and 892.

	Site 889 off Vancouver Island	Site 892 off Central Oregon
Water Depth (m)	1320	670
Geothermal gradient	54°C/km and linear. At both sites the gradient is compatible with conductive heat transfer.	51°C/km and linear
Depth of Seismic BSR (mbsf)	224	74
Maximum Cl dilution*	36%	15%
Base of pure H_2O–pure CH_4 gas hydrate stability field	At both sites at ~2°C higher than the temperature at the seismic BSR,or at a corresponding greater burial depth (greater pressure).	
CH_4 distribution	A coincidence between low Cl and high CH_4 headspace at both sites.	
Occurrence of "soupy" core intervals	Predominantly above 280 mbsf	Only above the BSR depth
Free gas	Present below the BSR depth At both sites inferred from low VSP velocity.	Present below the BSR depth

Note: * = Assuming bottom-water Cl concentration.

along the Cascadia subduction zone of up to 5 mm/yr was recorded by Mitchell et al., 1994). At least 50 to 100 m of tectonic uplift and sedimentation together with a ~70 m displacement caused by interglacial bottom-water warming, discussed in Westbrook, Carson, Musgrave, et al. (1994), indicates that an upward migration of the base of the stability field of gas hydrate (and BSR) of ≥120 m most probably has occurred over the past 10 to 15 millennia in the Cascadia margin. Accordingly, during the last glacial maximum, the base of the stability field (and BSR) at Site 889 is inferred to have been considerably deeper: at 300 to 350 mbsf at Site 889 instead of at ~224 mbsf, and at ~150 to 200 mbsf at Site 892 instead of at ~74 mbsf.

The most prominent geochemical consequences of the upward migration of the base of the gas hydrate stability field (and BSR) are the release of the guest gas from the hydrate cages, and of H_2O from the dissociation of the solid water clathrate. In most natural gas hydrates, methane is the dominant gas. Its solubility in seawater is very low (Yamamoto et al., 1976); therefore, methane supersaturation would ensue upon methane hydrate dissociation. It would require over 10^5 years to erase this geochemical perturbation, assuming regional upward fluid advection at a rate ≤1.0 mm/yr, caused by compaction of sediments with 50% porosity (Hyndman et al., 1993; Wang et al., 1993). Accordingly, in the Cascadia subduction zone, in regions with upward fluid advection resulting only from regional tectonic compaction, based on the above calculated ~120 m upward migration of the BSR since the last glacial maximum (18,000 yr BP), a 70- to 90-m-thick zone of diluted pore fluids might be anticipated underneath the modern BSR. The upward-migrating methane driven by the advection and buoyancy would form new hydrate above the BSR. Some of the released methane might be retarded by "trapping" as bubbles beneath the new BSR, but probably for relatively short geological periods, until the bubbles coalesce and migrate upward to form new hydrate. The formation of hydrate would cease only when all pore space is occupied by the hydrate. Regardless of the processes for attaining gas supersaturation, on the basis of thermodynamic considerations in simple two component systems, the Gibbs phase rule requires the presence of a gas phase at the base of the stability field of a gas hydrate zone.

Temperature of a Core Measured upon Retrieval

Further evidence for the presence of gas hydrate at Site 889 is provided by the lower-than-in situ temperature measured in Core 3R of Hole 889B at a depth of 217 mbsf immediately after recovery. The core temperature measured was –1.4°C. Excluding the heat exchange that occurred during recovery, the in situ temperature is higher by 14.4°C, given a geothermal gradient of 54°C/km. Cores are cooled, however, by passage through deep sea (~2°C) during recovery, accordingly the minimum cooling by hydrate dissociation is from 2° to –1.4°C. On the basis of the heat required to dissociate a unit volume of methane hydrate (Makogon, 1981; Sloan, 1990), the wet sediment heat capacity and the density of methane hydrate (0.92 g/cm^3), at 49% in situ porosity dissociation of ~3% of pore space hydrate occupancy would yield the observed temperature drop. Similar low temperatures were measured in cores that contained the solid CH_4-H_2S hydrate, at 2 to 19 mbsf at Site 892.

Chloride Concentration-depth Profiles across the BSRs

Chloride has usually been assumed to behave conservatively during diagenesis and metamorphism. Recent findings, involving chlorine stable isotope ratios, however, indicate that Cl is directly involved in hydrous silicate reactions, including clay mineral authigenesis and transformation reactions in subduction zones (Ransom et al., 1995). Nevertheless, Cl involvement in silicate reactions impacts only the baseline Cl concentration. Cl will be diluted or concentrated by gas hydrate dissociation or formation, respectively; therefore, Cl concentration depth profiles are highly effective for detecting recently dissociated gas hydrate. In addition to gas hydrate dissociation, other important reactions involving the release of water in subduction zones are hydrous silicate dehydration and/or transformation, membrane ion filtration, and mixing with meteoric water. Hydrous silicate formation is an important reaction involving the uptake of H_2O, as does gas hydrate formation. The residual fluid from clay membrane filtration is also saline. A detailed discussion of these reactions and their relation to Cl concentrations is given in Kastner et al. (1991).

Because methane hydrate is primarily composed of CH_4 and H_2O, the only significant geochemical consequences of its dissociation are: (1) the release of a large volume of methane (at STP the volumetric ratio of H_2O/CH_4 of a saturated methane hydrate $CH_4 \cdot 5¾\ H_2O$ is 1/164 [Davidson et al., 1978; Sloan, 1990]); (2) the release of fresh water; and (3) the fresh water released contains heavier values of the oxygen and hydrogen isotopes than the pore fluid with which it mixes. The isotope behavior during formation of gas hydrate is closely analogous to the formation of sea ice. Experimentally derived fractionation factors for oxygen for the ice-water system range from 1.0031 to 1.0027 (O'Neil, 1968; Suzuki and Kimura, 1973, Craig and Hom, 1968. However, only Craig and Hom (1968) studied the formation of sea ice and derived the fractionation factor of 1.0027. Their value is closest to that of Davidson et al. (1983), who determined directly the ^{18}O enrichment of gas hydrate to be 1.0026. For hydrogen, the experimentally derived fractionation factor for the ice-water system ranges from 1.0235 to 1.0195 (Merlivat and Nief, 1967; O'Neil, 1968; Craig and Hom, 1968; Arnason, 1969). The only natural gas hydrate from a subduction zone analyzed for its H_2O oxygen and hydrogen isotopic compositions is a methane hydrate sample from the Peru subduction zone. Its extrapolated $\delta^{18}O$ value is 2.4‰ and δD value is 21.8‰ (Kvenvolden and Kastner, 1990). These values lie approximately within the ranges of the above experimental values, suggesting a similar mode of formation. The remaining chemical components in the pore fluids will be simply diluted by the same proportion as Cl concentrations; thus normalization to Cl concentration should result in no shifts. Clearly, isotopic ratios, such as Sr, should not be affected by the dilution.

Chloride concentration-depth profiles from Sites 889 and 892, although strikingly different, clearly show significant Cl dilution at various depth intervals (Fig. 2). Both sites lie within the methane hydrate stability field from the seafloor to the depths of their BSRs.

Site 889/890

At Site 889, the Cl diffusion profile in the uppermost 130 m is primarily controlled by a low-Cl fluid conduit at ~130 mbsf (Figs. 2 and 3) (Kastner et al., this volume; Westbrook, Carson, Musgrave, et al., 1994), which is not directly related to the gas hydrate-BSR relationship dealt with in this paper, and thus will not be discussed further. The almost constant low Cl concentration of 362 ± 10 mM, mostly between 190 to ~310 mbsf, suggests either gas hydrate dissociation upon core recovery or advection of a low-Cl fluid from >1 to 3 km depth, at which clay mineral transformation and dehydration reactions occur along the 54°C/km geothermal gradient (Perry and Hower, 1972). Dilution as a result of mixing with meteoric water is not supported by the geological setting of this site, and the very low efficiency of the membrane ion filtration process excludes it as an important factor in such a considerable dilution. Evidence from depth profiles of other chemical concentrations given in Westbrook, Carson, Musgrave, et al. (1994), normalized to Cl in Tables 2 and 3 and Figure 2, suggests dilution by gas hydrate as the most plausible origin for much of the Cl dilution between 190 to ~310 mbsf. Furthermore, as discussed below and in Westbrook, Carson, Musgrave, et al. (1994), the extension of the low-Cl zone below the BSR, at 224 mbsf, suggests that it most likely represents an integrated modern and last glacial methane hydrate zone. Porosity variations with depth between 42% and 56% (Westbrook, Carson, Musgrave, et al., 1994) could

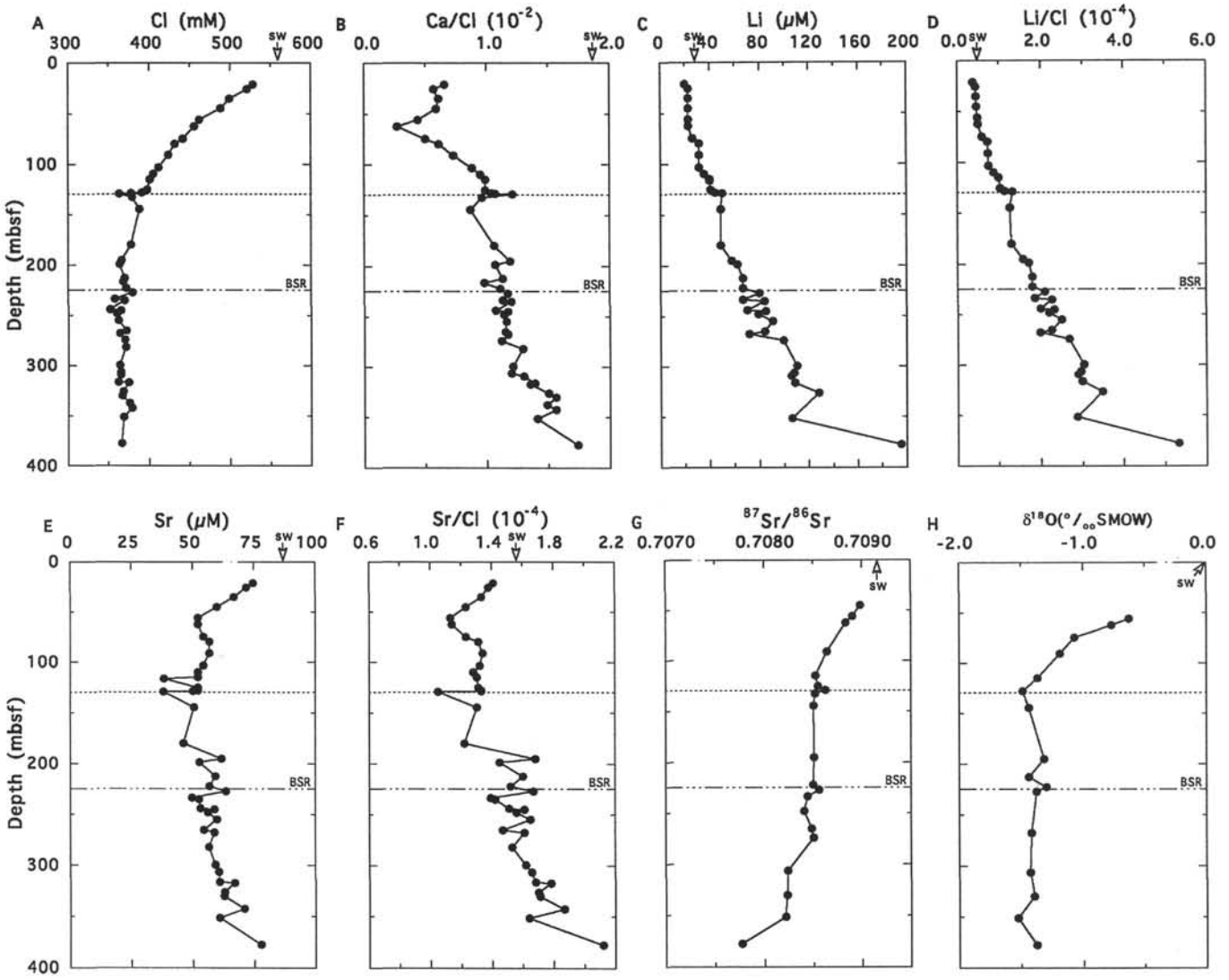

Figure 2. Depth profiles of pore fluid chemical composition (A–F) and isotopic composition (G–H) from Site 889. **A.** Cl concentrations. **B.** Ca/Cl ratios. **C.** Li concentrations. **D.** Li/Cl ratios. **E.** Sr concentrations. **F.** Sr/Cl ratios. **G.** $^{87}Sr/^{86}Sr$ ratios. **H.** $\delta^{18}O$ (‰ SMOW) values. Arrow indicates seawater composition. Dotted line represents the conduit at ~130 mbsf.

easily account for the observed ±10 mM in Cl concentrations within this depth interval.

In addition, the coincidence of low chlorinity with high concentrations of headspace methane (Fig. 3A) supports the conclusion that chiefly methane hydrate is present at this site. Its dissociation during core recovery apparently is responsible for most of the observed chemical dilutions and for much of the high methane concentrations.

The extent of Cl dilution would indicate the amount of gas hydrate present, if the baseline chemistry were known, which is not the case for this site. Assuming a bottom-water Cl concentration of 548 mM, (derived by extrapolating the Cl profile of Figure 2 to the seafloor), dilution to 362 mM at ~50% porosity and 0.92 g/cm^3 methane hydrate density, implies that 37% of the pore space must have been occupied by gas hydrate. As discussed earlier, the geophysical evidence suggests pore space occupancy of ~15%. Although pore fluids with lower-than-seawater Cl concentrations are ubiquitous in accretionary prisms, ~35% seawater dilution was previously observed only once, in the Middle America Trench, during DSDP Leg 84 (Hesse et al., 1985). There a large mass of gas hydrate was recovered, and only a fraction of it dissociated during core recovery operations.

Adopting a pore space methane hydrate occupancy of a minimum of 15% and assuming initial pore fluid Cl concentration equal to the bottom-water concentration of 548 mM, the dissociation of all the hydrate would have lowered the Cl concentration to 466 mM; instead, the observed value is 362 ± 10 mM (Table 2), that is, 104 mM too low. On the other hand, if the in situ pore fluid Cl concentration is 420 mM, fresher than bottom water by 126 mM Cl, the dissociation of methane hydrate, which occupies 15% of the pore space, at 50% porosity would lower the pore-fluid Cl concentration to the observed 362 mM. An in situ Cl baseline of 420 mM suggests that other processes have previously diluted it. Diffusional communication with the overlying low-Cl fluid aquifer at 130 mbsf is a plausible process. At 50% porosity and a formation factor of ~8 (Westbrook, Carson, Musgrave, et al., 1994) the calculated sediment diffusion coefficient (Ds) is 2.5×10^{-6} cm^2 s^{-1}. Accordingly, diffusional communication from ~130 mbsf to the depth of the BSR would require 700 millennia, and almost 2 m.y., to reach ~310 mbsf. This time is longer than the accretion time available at this margin of ~1 m.y. (Westbrook, Carson, Musgrave, et al., 1994). At Ds = 2.5×10^{-6} cm^2 s^{-1} the diffusion path length over 1 m.y. is ~120 m, from 130 mbsf to a maximum depth of 250 mbsf. Therefore, an additional low-Cl fluid source must exist at greater depth.

If pore space occupancy by methane hydrate is approximately 15%, then supersaturation with respect to methane solubility will occur upon hydrate dissociation. The oxygen isotopic composition of the pore fluid would, however, be influenced by a maximum of 0.4‰

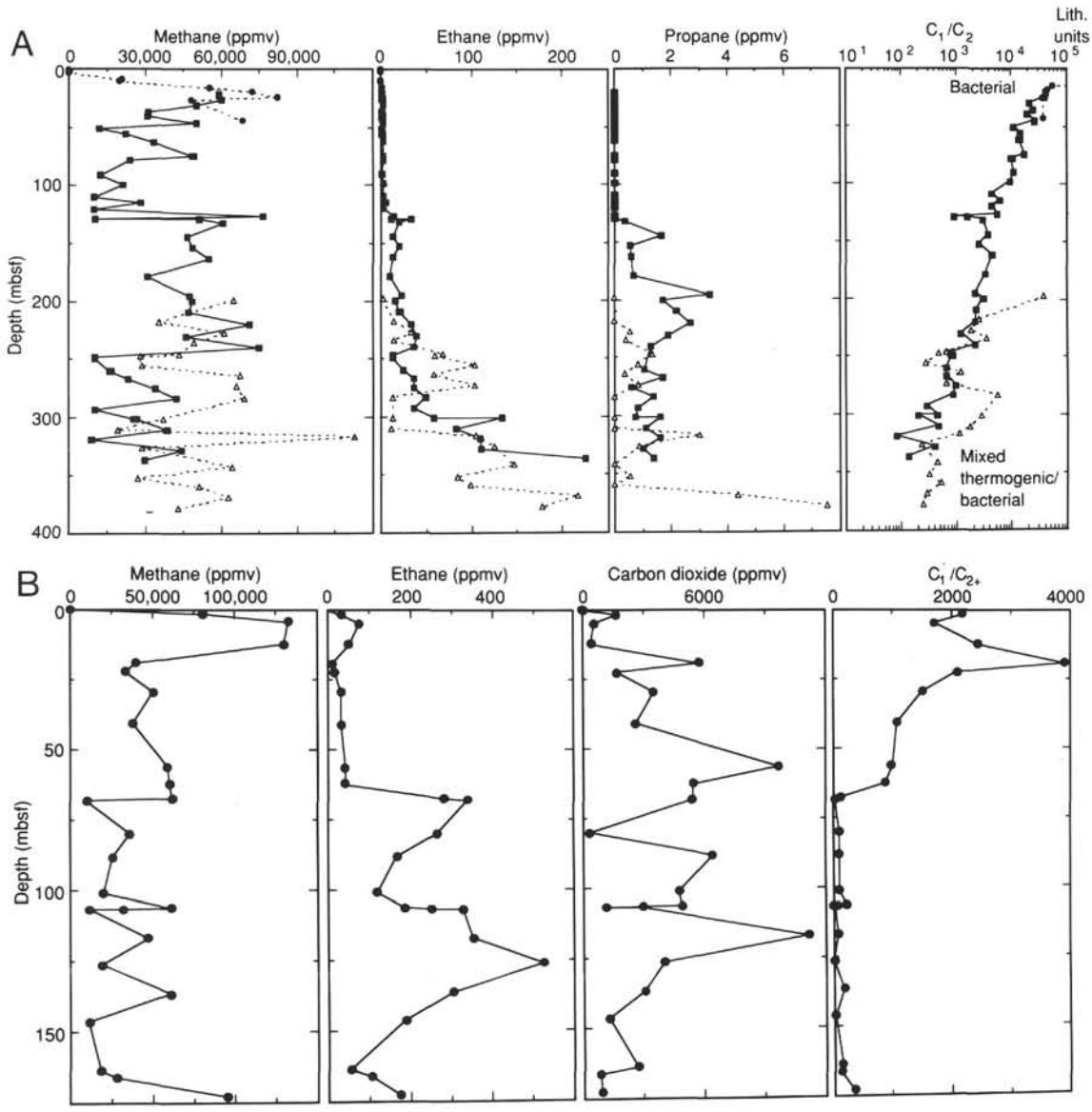

Figure 3. Depth profiles from **(A)** Site 889 and **(B)** Site 892, showing concentrations of methane, ethane, propane or CO_2, and C_1/C_2 ratios (from Westbrook, Carson, Musgrave, et al., 1994).

at 50% porosity. Such a small change in isotopic composition could be difficult to recognize in pore fluids altered isotopically by diagenesis.

The above calculations suggest that a minimum of one-third of the Cl dilution observed between 190 to ~310 mbsf has been generated by dissociation of the Holocene and older gas hydrates. This conclusion is supported by the chemical and isotopic composition depth profiles, shown in Figures 2 and 3, in Tables 2 and 3, and in Westbrook, Carson, Musgrave, et al. (1994). Most of the remaining observed dilution above the BSR has originated from diffusional communication with the low-Cl aquifer at ~130 mbsf (whose origin most likely is also related to gas hydrate dissociation at its source region), and below 310 mbsf, from communication with a deeper-source low-Cl fluid. The geochemical, isotopic (O, Sr) and hydrocarbons depth profiles (Figs. 2, and 3) indicate that fluids have migrated by dispersive (non-channelized) flow from a depth where thermogenic hydrocarbons are being generated. Given a geothermal gradient of 54°C/km, such a depth occurs at >1.5 to <4 km. In order to remain consistent with a linear geothermal gradient, the flow rate must be ≤1–2 mm/yr. The aquifer at ~130 mbsf acts as a barrier to this dispersive flow; no allochthonous thermogenic hydrocarbons exist above it (Whiticar et al., this volume., and Fig. 3). Even though the Sr isotope values throughout the section are less radiogenic than those of modern seawater or of the contemporaneous marine sediments (Table 3 and Fig. 2), the source of the Sr above the aquifer is the nonradiogenic aquifer fluid, not the deeper-source fluid.

The fluid from the deeper-source is geochemically different, is characterized by low Cl and Mg concentrations, elevated Ca and silica concentrations, higher (Ca/Cl), Li (Li/Cl), Sr (Sr/Cl), ratios, higher, light (negative) oxygen isotopes, and nonradiogenic Sr isotopes. The Sr-isotope values of the pore fluids, which are solely representative of sources and sinks, and the depth distribution of the thermogenic hydrocarbons ethane and propane beneath the 130 mbsf aquifer, clearly divide this low-Cl section into three domains (Figs. 2–4): from 130 mbsf to the BSR depth the Sr isotope ratios remain basically constant, and the ethane and propane concentrations are very low, probably too low for structure II hydrate to form. Because the source of the elevated N_2 concentrations observed at and near the depth of the BSR (Westbrook, Carson, Musgrave, et al., 1994) is uncertain, whether a component of the in situ gases or from air contamination,

Table 2. Chemical composition of pore fluid samples from Site 889.

Core, section, interval (cm)	Depth (mbsf)	Cl (mM)	Ca/Cl (10^{-2})	Li (μM)	Li/Cl (10^{-4})	Sr (μM)	Sr/Cl (10^{-4})
146-889A-							
1H-2, 1–6	21.6	528	0.66	19.8	0.38	74.7	1.41
1H-4, 145–150	26.0	521	0.57	22.7	0.44	71.8	1.38
2H-5, 145–150	35.5	499	0.61	22.7	0.45	66.5	1.33
3H-5, 1–6	45.0	488	0.59	22.7	0.47	59.8	1.23
4H-5, 143–150	56.0	462	0.44	22.7	0.49	52.0	1.13
5H-3, 143–150	62.5	456	0.27	22.7	0.50	52.0	1.14
6H-5, 145–150	75.0	442	0.50	26.6	0.60	54.4	1.23
7H-2, 143–150	80.0	432	0.61	31.5	0.73	56.7	1.31
8H-3, 140–150	91.0	424	0.73	31.5	0.74	56.7	1.34
9H-6, 137–150	103.4	412	0.88	31.5	0.76	54.4	1.32
10H-4, 140–150	109.9	405	0.95	35.8	0.88	52.0	1.28
11H-1, 140–150	115.0	401	0.99	40.2	1.00	52.0	1.30
11H-2, 130–150	116.4			40.2		38.4	
12H-4, 140–150	125.0	398	0.99	41.0	1.03	52.0	1.31
13H-CC, 0–5	128.0	391	1.04	44.6	1.14	52.0	1.33
14H-1, 153–158	128.5	378	1.07	50.0	1.32	50.1	1.33
15P-1, 6–13	129.1	363	1.21			38.1	1.05
17X-2, 70–80	132.4	379	0.96				
18X-4, 36–46	144.5	388	0.87	49.0	1.26	50.4	1.30
22X-7, 0–20	179.8	378	1.06	49.0	1.30	46.3	1.22
24X-5, 120–140	195.1	366	1.19	57.9	1.58	61.5	1.68
25X-2, 0–20	198.8	364	1.07	62.4	1.71	52.7	1.45
26X-4, 130–150	212.7	370	1.13	66.5	1.80	59.2	1.60
28X-4, 80–100	222.6	372	1.11	66.5	1.79	56.7	1.52
30X-4, 130–150	233.7	358	1.13	66.5	1.86	49.7	1.39
31X-5, 140–160	244.0	352	1.07	70.0	1.99	53.2	1.51
32X-1, 130–150	248.0	360	1.14	78.8	2.19	56.1	1.56
36X-1, 99–114	267.7	364	1.17	71.7	1.97	58.7	1.61
40X-4, 45–65	306.6	365	1.20	107.9	2.96	60.5	1.66
41X-3, 130–150	316.4	362	1.39	108.4	2.99	60.8	1.68
43X-2, 0–5	329.9	367	1.56			62.6	1.71
44X-1, 0–15	337.3	376	1.49				
146-889B-							
3R-1, 79–94	216.5	368	0.98				
4R-2, 45–60	227.3	380	1.17	79.9	2.10	63.3	1.67
5R-1, 26–36	235.1	370	1.20	84.0	2.27	52.5	1.42
6R-1, 54–69	244.9	365	1.17	84.7	2.32	58.7	1.61
7R-1, 103–126	255.0	362	1.16	90.6	2.50	59.8	1.65
8R-2, 130–150	265.6	372	1.15	84.0	2.26	54.5	1.47
9R-1, 130–150	274.3	370	1.12	99.2	2.68		
10R-2, 0–20	282.0	371	1.29			56.6	1.53
12R-1, 130–150	299.6	364	1.21	110.3	3.03	59.1	1.62
13R-2, 35–55	309.1	365	1.30	105.9	2.90		
14R-1, 111–136	317.0	375	1.35			66.8	1.78
15R-1, 125–150	326.0	368	1.50	127.8	3.47	62.7	1.70
17R-1, 0–15	342.2	379	1.56			70.9	1.87
18R-1, 0–10	351.1	369	1.41	106.0	2.87	60.7	1.64
20R-CC, 0–3	377.6	366	1.74	195.2	5.33	77.6	2.12

its potential role in controlling the hydrate structure type is not considered here. Between the BSR and ~310 mbsf, $^{87}Sr/^{86}Sr$ ratios decrease slowly with depth and become less radiogenic, whereas ethane concentrations increase. Below ~310 mbsf, $^{87}Sr/^{86}Sr$ ratios decrease more sharply, and ethane and propane concentrations rapidly increase with depth (Kastner et al., this volume; Whiticar et al., this volume). This division implies that the deeper-source fluid carrying thermogenic hydrocarbons has little influence on the pore fluids above the BSR or on the gas hydrate composition. Between the BSR and ~310 mbsf, the influence of the deep-source fluid increases, and below ~310 mbsf pore fluid is strongly influenced by fluid which has migrated from >1.5 km depth. On the basis of the geothermal gradient, the light oxygen isotopic composition of this fluid suggests that its origin is from ~2 but <3 km depth (Lawrence et al., 1975), adequate for thermogenic hydrocarbon generation. Heavier oxygen isotopes would characterize a fluid originating from >3 km depth. The above subdivision of the section into three geochemical domains, with only the shallowest one related to modern gas hydrate, is further supported by most inorganic and organic chemical data, provided that, since the last glacial maximum, the base of the stability field (and BSR) has migrated upward by ≥120 m.

Site 892

At Site 892 the distinctly non-steady-state Cl concentration profile, characterized by closely spaced concentration reversals particularly above the BSR, is superimposed on an overall decrease of Cl concentrations with depth. Although in Hole 892C the BSR was determined to be at 74 mbsf (Mackay et al., 1994), on the basis of geochemical evidence from Figures 3B and 5 and Table 4, it must be at ~68 mbsf in Hole 892A. This offset is not surprising for a strongly faulted section; other offsets between the various holes drilled at this site exist (Westbrook, Carson, Musgrave, et al., 1994). The strongest Cl dilution and highest methane concentrations observed in the uppermost ~20 mbsf are related to the dissociation of an H_2S-rich methane hydrate partially recovered at this site (Kastner et al., unpubl. data). It is, however, important to note the clear influence a dissociating, dominantly methane hydrate has on the pore fluid geochemistry: Cl concentrations, as well as all other components analyzed, are significantly lower than the corresponding seawater concentrations because of dilution by H_2O released, methane concentrations are extremely high, and the $\delta^{18}O$ values are less negative (Figs. 3B and 5, Tables 4–6).

Above the BSR, between ~20 to 68 mbsf, three narrow (1–2-m-wide) low-Cl intervals, at ~30, ~56, and 68 mbsf, are seen in Fig. 5. The extent of dilution increases with depth, from 9% at 30 mbsf, to 11% at ~56 mbsf, and to approximately 15% seawater dilution at 68 mbsf, the depth of the BSR. Below the BSR, the Cl and other geochemical depth profiles are considerably smoother, although less pronounced Cl minima occur at ~88, ~106, and 136 mbsf. Were any of these 3 deeper Cl-minima generated by paleo-gas–hydrate dissociation, or do they manifest advective flow? The limited vertical extent of the Cl-minima intervals, a maximum of 2 m, precludes the possibility of having paleo-gas–hydrate intervals below the BSR. With a diffusion coefficient of 3×10^{-6} cm^2 s^{-1}, derived based on 55% poros-

Table 3. Isotopic composition of pore fluid samples from Leg 146, Site 889.

Core, section, interval (cm)	Depth (mbsf)	Sr (μM)	$^{87}Sr/^{86}Sr$	2σ	$\delta^{18}O$ (‰ SMOW)
146-889A-					
3H-5, 1–6	45.0	59.8	0.708977	19	
4H-5, 143–150	56.0	52.0	0.708899	16	−0.63
5H-3, 143–150	62.5	52.0	0.708826	18	−0.77
6H-5, 145–150	75.0	54.4			−1.07
8H-3, 140–150	91.0	56.7	0.708637	20	−1.19
11H-1, 140–150	115.0	52.0	0.708521	18	−1.37
12H-4, 140–150	125.0	52.0	0.708544	18	
13H-CC, 0–5	128.0	52.0			−1.49
15P-1, 6–13	129.1	38.1	0.708622	17	
17X-2, 70–80	132.4		0.708514	15	
18X-4, 36–46	144.5	50.4	0.708497	17	−1.44
24X-5, 120–140	195.1	61.5	0.708507	16	−1.32
26X-4, 130–150	212.7	59.2			−1.44
28X-4, 80–100	222.6	56.7	0.708492	16	−1.30
146-889B-					
4R-2, 45–60	227.3	63.3	0.708554	18	−1.38
146-889A-					
30X-4, 130–150	233.7	49.7	0.708438	18	
32X-1, 130–150	248.0	56.1	0.708402	16	
146-889B-					
8R-2, 130–150	265.6	54.5	0.708477	19	
146-889A-					
36X-1, 99–114	267.7	58.7			−1.42
146-889B-					
9R-1, 130–150	274.3		0.708449	15	
146-889A-					
40X-4, 45–65	306.6	60.5	0.708237	18	−1.43
43X-2, 0–5	329.9	62.6	0.708224	16	−1.40
146-889B-					
18R-1, 0–10	351.1	60.7	0.708213	18	−1.53
20R-CC, 0–3	377.6	77.6	0.707766	19	-1.38

ity and a formation factor of 6 (Westbrook, Carson, Musgrave, et al., 1994), with no advection a 2-m-wide low-Cl interval would disappear in 50 to 60 yr. On the other hand, the depths of the lower three distinct Cl-minima are fault zones, which serve as active fluid conduits, as discussed in Westbrook, Carson, Musgrave, et al. (1994). At ~88 mbsf a 2.5°C temperature anomaly occurs, and strong thermogenic hydrocarbon peaks occur at the other two intervals (Fig. 3B).

Above the BSR, from ~20 to 68 mbsf, other depth profiles of major ions (Na, K, Ca, and Mg) exhibit concentration minima at the same three depths as the Cl minima (Westbrook, Carson, Musgrave, et al., 1994). At the 30 and 56 mbsf intervals, the smooth normalized-to-Cl depth profiles (Fig. 5), indicate that these other components exhibit dilutions equivalent to those reflected by Cl. In addition, in the adjacent Hole 892D at 28 mbsf, a core temperature of 0.9°C was measured, which, at a geothermal gradient of 51°C/km and 4.7°C bottom water temperature, is 5.2°C lower than the in situ temperature, and 3.6°C lower than the bottom water temperature, suggesting that 3% to 4% of the pore space was filled with gas hydrate that dissociated. These low-Cl intervals are associated with "soupy" layers; no discontinuities in physical properties nor faults have been identified at the 30 and 56 mbsf Cl minima. Therefore, chemical anomalies of at least the two uppermost Cl-minimum intervals must have been generated from small local concentrations of gas hydrate that dissociated upon core recovery. The chemical baseline is unknown and cannot be extrapolated to the seafloor because of the pore-fluid anomalies in the uppermost ~20 mbsf resulting from the partial dissociation of the H_2S-rich methane hydrate. Hence, the volume of pore-space occupied by the gas hydrate could not be calculated. An estimate of ≤10% hydrate volume is made on the basis of seawater dilution calculations. Specific lithologic horizons probably favor the formation of gas hydrate. More such hydrate intervals may exist, based on the frequency of occurrence of "soupy" layers that are confined to the depth interval above the BSR (Fig. 6), but most were not sampled for pore fluid chemistry. The high methane concentration throughout this depth interval (Fig. 3B) is consistent with this conclusion.

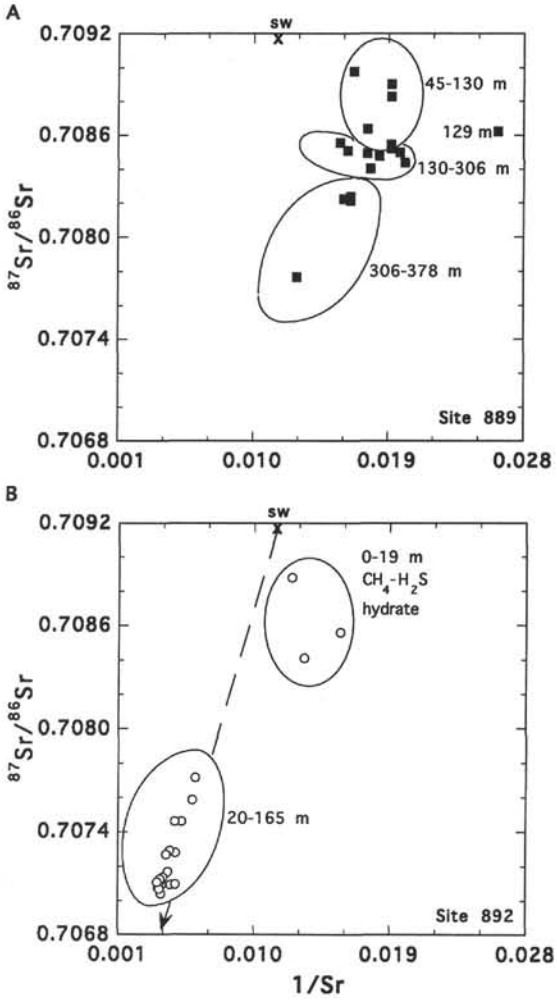

Figure 4. Mixing relationships between $^{87}Sr/^{86}Sr$ ratios and 1/Sr concentrations from **(A)** Site 889 and **(B)** Site 892. The delineated areas divide the sections into geochemical domains, discussed in the text.

The low-Cl interval at 68 mbsf, in a "soupy" layer, has the most intense Cl minimum, is located just above the BSR, and is associated with a 1.6°C temperature anomaly and discontinuities in physical properties. Also, high concentrations of thermogenic hydrocarbons from ethane through hexane, shown in Fig. 3B, occur here. The normalized-to-Cl Na, Ca, and Mg profiles have maxima and minima respectively at this depth, indicating that simple dilution by H_2O cannot be the only process responsible for the observed maximum 15% seawater dilution at this depth interval. Mixing with a warmer advecting fluid from greater depth that carries with it the thermogenic hydrocarbons is suggested; the warm fluid may destabilize the in situ gas hydrate.

In summary, channelized advective fluid migration from a deeper source where thermogenic hydrocarbons are produced, dominates the geochemistry of the section below the BSR. The fluid is enriched in Sr and Li and is characterized by nonradiogenic Sr isotopes and slightly negative oxygen isotopes (Figs. 3B, 4, and 5, Tables 4, 6). Above the BSR, but below ~20 mbsf (below the CH_4–H_2S hydrate recovered at 2 to ~19 mbsf), small amounts (<10%) of disseminated,

Table 4. Chemical composition of pore fluid samples from Site 892.

Core, section, interval (cm)	Depth (mbsf)	Cl (mM)	Ca/Cl (10^{-2})	Li (μM)	Li/Cl (10^{-4})	Sr (μM)	Sr/Cl (10^{-4})
146-892A-							
1X-5, 10–13	6.1	483	0.70	28.4	0.59	70.7	1.46
2X-3, 0–11	12.6	468	0.90	28.7	0.61	75.4	1.61
3X-2, 0–10	20.6	557	1.00	66.7	1.20	164.3	2.95
3X-3, 0–10	22.1	552	0.80	71.6	1.30	159.6	2.89
4X-2, 0–10	30.1	523	1.00	84.3	1.61	169.0	3.23
6X-2, 0–10	40.6	544	1.00	110.3	2.03	192.4	3.54
6X-2, 10–30	40.7	545	1.10	116.4	2.14	199.4	3.66
7X-5, 140–150	55.9	507	1.20	143.4	2.83	208.7	4.12
8X-3, 0–10	61.0	534	1.20	155.8	2.92	229.8	4.30
9X-1, 69–74	68.2	480	1.30			232.7	4.85
11X-2, 0–10	79.6	517	1.30	176.3	3.41	267.2	5.17
11X-2, 70–95	80.3	516	1.40	186.8	3.62	262.5	5.09
12X-1, 0–7	87.5	489	1.50			245.0	5.02
13X-4, 0–25	101.6	504	1.40	188.4	3.74	259.4	5.15
13X-6, 69–82	105.3	501	1.40	161.6	3.23	213.2	4.26
14X-1, 35–38	106.9	491	1.60	215.3	4.38	234.8	4.78
15X-1, 88–100	116.9	497	1.40	168.5	3.39	223.7	4.50
16X-1, 34–43	125.8	493	1.40	168.3	3.41	260.2	5.28
17X-2, 3–13	136.6	481	1.40	156.3	3.25	207.5	4.31
18X-1, 115–140	145.8	487	1.40	167.9	3.45	264.9	5.44
18X-1, 140–150	146.0	487	1.40	161.0	3.31	260.2	5.34
20X-2, 0–10	165.1	489	1.40	156.9	3.21	278.9	5.70
20X-3, 0–10	166.5	496	1.40	154.0	3.11	261.4	5.27
146-892D-							
1X-1, 9–12	0.1	547	1.80	33.3	0.61	87.1	1.59
2X-1, 145–150	10.0	539	0.60	31.2	0.58	80.1	1.49
2X-2, 140–150	11.4	447	0.70	27.8	0.62	63.7	1.43
3X-1, 40–45	18.4	433	0.80	28.8	0.67	54.2	1.25
4X-2, 4–11	29.0	575		82.0	1.43	161.7	2.81
4X-2, 21–30	29.2	505	1.00	61.0	1.21	131.3	2.60
4X-3, 80–88	30.8	570		84.1	1.48	180.7	3.17
5X-2, 140–150	39.9	560	1.00	104.3	1.86	197.0	3.52
6X-4, 140–150	52.4	550	1.10	126.7	2.30	211.1	3.84
7X-3, 142–150	58.2	551	0.70	147.2	2.67	234.5	4.26
8X-3, 0–10	64.7	541	0.80	154.7	2.86	239.1	4.42
9X-4, 0–15	73.8	500	0.90	163.0	3.26	250.8	5.02
10X-4, 0–15	104.5	496		175.2	3.53	273.7	5.52
11X-1, 130–150	110.9	505	0.90	170.7	3.38	277.0	5.49
12X-3, 130–150	123.4	488	0.90	165.2	3.39	260.2	5.33
13X-CC, 22–24	128.5	484				272.9	5.64
14X-1, 115–130	139.2	490	0.80	156.8	3.20	267.2	5.45
15X-2, 110–135	148.6	489	1.00	160.5	3.28	246.2	5.03
15X-2, 135–150	148.9	492	0.80	147.7	3.00	267.2	5.43
16X-3, 135–150	161.4	484	0.70	141.0	2.91	267.2	5.52
16X-5, 135–150	164.4	485	0.80	136.4	2.81	267.2	5.51

mainly methane hydrate are concentrated along specific sediment horizons. The warm fluid flowing along the BSR depth horizon at ~68 mbsf may destabilize the in situ gas hydrate, cause the release of its caged gases, and thus supersaturate the associated pore fluid with methane. It seems that geophysical data are not sensitive enough to detect the presence of ≤10% of disseminated hydrate.

Depth Distribution of Unusually Wet, "Soupy" Sediment Intervals

Numerous unusually wet, "soupy" sediment intervals, some of which are sandy, are sandwiched between undisturbed "normal" sediment sections. The layers often consist of a fluidized, homogeneous mixture of sediment and water with dispersed fragments of firm sediment. A slight increase in the mean size of the bulk sediment has been noted across some intervals at Site 892. The thickness of the soupy layers is usually less than 1 m (lower than 0.6 m at Site 892) and interspacing varies from 1 to 6 m. At Site 889 "soupy" layers occur above the BSR and a few also occur in the inferred paleo-hydrate zone below the BSR. At Site 892, all of the "soupy" intervals occur above the BSR, none below (Fig. 6). The pore fluids of several pairs of "soupy" and adjacent "normal" sediment intervals were analyzed, especially for Cl and sulfate concentrations. Dissolved sulfate is one of the most sensitive indicators of drilling contamination (by surface seawater) in reduced sediment sections, and Cl concentrations are used for determining the extent of pore water dilution. Surface seawater (the drilling water) was analyzed at both sites, providing necessary information for baseline corrections, because "soupy" intervals are more prone to drilling contamination than are normal, undisturbed sediment intervals. The results clearly indicated excess Cl dilution of the pore fluids of the "soupy" layers, as discussed in Westbrook, Carson, Musgrave, et al. (1994). The only available in situ dilutant appears to be gas hydrate; because of hydrate dissociation upon core recovery these sediment intervals apparently become liquefied.

Gas Composition

On the basis of the gas chemistry the gas hydrate associated with the BSRs is primarily a methane hydrate, possibly including some CO_2 and ethane as suggested in Fig. 3. The gas chemistry is discussed in detail in Whiticar et al., this volume.

Which Gas Hydrate Stability Field Do the Cascadia Margin BSRs Represent?

Pressure and temperature (P–T) conditions of the pure H_2O–pure CH_4 hydrate system have been investigated extensively from a large range of natural environments including permafrost to subduction zone accretionary complexes (Platteeuw and Van der Waals, 1958; Van der Waals and Platteeuw, 1959; Katz et al., 1959; Miller, 1974; Sloan, 1990, and references therein). The effects of mixing with other gases and of electrolyte solutions on the P–T conditions have been investigated over a narrower range of natural environments (e.g., Englezos and Bishnoi, 1988; Sloan, 1990; Dholabhai et al., 1991; Dickens and Quinby-Hunt, 1994, and references therein). Therefore, these conditions need to be extrapolated to the typical P–T conditions prevailing in subduction zones. As shown in Figure 7, at least at pressures of <100 MPa, the addition of CO_2 increases the maximum temperature of hydrate formation, whereas the addition of NaCl depresses it. On the basis of thermodynamic considerations Englezos and Bishnoi (1988) predicted that by adding simple salts to water the sequence of intensity of depression of the methane hydrate formation temperature is $CaCl_2$ > KCl > NaCl. Experiments have shown similar salt effects (Katz et al., 1959; Menton et al., 1981; Sloan, 1990; Dholabhai et al., 1991). Recently, Dickens and Quinby-Hunt (1994) conducted experiments on methane hydrate stability in seawater between 2.75 to 10 MPa pressure. They showed that throughout this pressure range the stability field is depressed approximately by a constant 1.1°C relative to the pure H_2O–pure CH_4 stability field. No experimental data at >10-MPa pressures exist for the seawater-methane hydrate stability field. The experimental data obtained by Dholabhai et al. (1991) in an artificial electrolyte solution resembling seawater are in agreement with the results obtained by Dickens and Quinby-Hunt (1994) for the seawater-methane hydrate stability field.

On the basis of the above experiments and theoretical considerations, it would be predicted that in the oceanic environment the stability field of the predominantly methane hydrate (Kvenvolden and McMenamin, 1980; Kvenvolden, 1988) should correspond with the experimental seawater-methane stability field. Good field calibrations of the temperature of the BSR are, however, difficult to obtain. On the basis of the limited available temperature data from the Blake-Bahama Outer Ridge and Peru and Nankai Trough accretionary complexes, Hyndman et al. (1992) concluded that the estimated P–T of the BSR at these sites best fit the base of the pure H_2O–pure CH_4 hydrate stability field. The measurement uncertainties, however, encompass the seawater stability field. If the difference between the seawater-methane system and the pure H_2O–pure CH_4 system indeed remains constant at ~1.1°C to 60 to 70 MPa, equivalent to 5 to 6 km water depth, the cases of correspondence with the pure H_2O–pure CH_4 base of the stability field (Fig. 7) may be simply a consequence of the uncertainties in acquired or extrapolated P–T data, or result

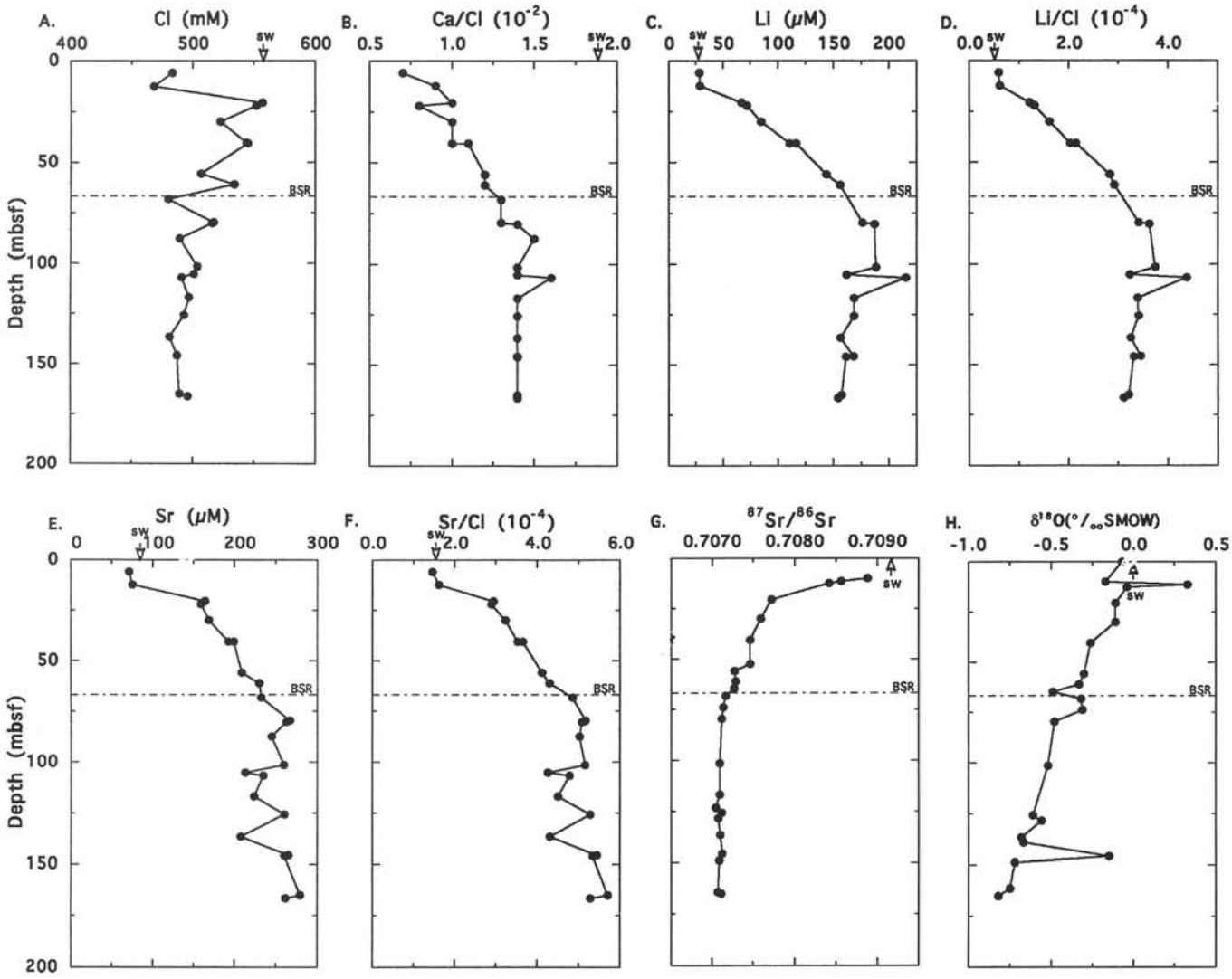

Figure 5. Depth profiles of pore fluid chemical composition (A–F) and isotopic composition (G–H) from Site 892. **A.** Cl concentrations. **B.** Ca/Cl ratios. **C.** Li concentrations. **D.** Li/Cl ratios. **E.** Sr concentrations. **F.** Sr/Cl ratios. **G.** $^{87}Sr/^{86}Sr$ ratios. **H.** $\delta^{18}O$ (‰ SMOW) values. Arrow indicates seawater composition.

Table 5. Chemical composition of pore fluid samples from Hole 892D.

Core, section, interval (cm)	Depth (mbsf)	Cl (mM)	Ca (mM)	Ca/Cl (10^{-2})	Mg (mM)	K (mM)	Na (mM)	Li (μM)	Li/Cl (10^{-4})	Sr (μM)	Sr/Cl (10^{-4})
146-892D-											
1X-1, 9–12	0.1	547	9.68	1.80	49.42	13.10	474	33.3	0.61	87.1	1.59
2X-1, 145–150	10.0	539	3.37	0.60	39.93	12.62	461	31.2	0.58	80.1	1.49
2X-2, 140–150	11.4	447	2.90	0.70	30.75	10.62	388	27.8	0.62	63.7	1.43
3X-1, 40–45	18.4	433	3.26	0.80	31.81	10.70	376	28.8	0.67	54.2	1.25
4X-2, 4–11	29.0	575				10.87		82.0	1.43	161.7	2.81
4X-2, 21–30	29.2	505	5.07	1.00	32.93	10.01	441	61.0	1.21	131.3	2.60
4X-3, 80–88	30.8	570				10.85		84.1	1.48	180.7	3.17
5X-2, 140–150	39.9	560	5.56	1.00	33.97	10.23	495	104.3	1.86	197.0	3.52
6X-4, 140–150	52.4	550	5.91	1.10	32.52	9.70	479	126.7	2.30	211.1	3.84
7X-3, 142–150	58.2	551	3.66	0.70	31.92	9.40	486	147.2	2.67	234.5	4.26
8X-3, 0–10	64.7	541	4.10	0.80	28.97	9.05	481	154.7	2.86	239.1	4.42
9X-4, 0–15	73.8	500	4.64	0.90	23.71	7.66	448	163.0	3.26	250.8	5.02
10X-4, 0–15	104.5	496				5.90		175.2	3.53	273.7	5.52
11X-1, 130–150	110.9	505	4.67	0.90	21.31	6.67	459	170.7	3.38	277.0	5.49
12X-3, 130–150	123.4	488	4.20	0.90	21.48	6.55	445	165.2	3.39	260.2	5.33
13X-CC, 22–24	128.5	484								272.9	5.64
14X-1, 115–130	139.2	490	3.94	0.80	21.59	6.53	447	156.8	3.20	267.2	5.45
15X-2, 110–135	148.6	489	4.81	1.00	21.85	6.88		160.5	3.28	246.2	5.03
15X-2, 135–150	148.9	492	4.00	0.80	21.45	6.50	451	147.7	3.00	267.2	5.43
16X-3, 135–150	161.4	484	3.56	0.70	21.96	6.47	442	141.0	2.91	267.2	5.52
16X-5, 135–150	164.4	485	3.78	0.80	21.43	6.36	444	136.4	2.81	267.2	5.51

Table 6. Isotopic composition of pore fluid samples from Site 892.

Core, section, interval (cm)	Depth (mbsf)	Sr (μM)	$^{87}Sr/^{86}Sr$	2σ	$\delta^{18}O$ (‰ SMOW)
146-892D-					
1X-1, 9–12	0.1	87.1			–0.07
1X-1, 145–150	10.0	80.1	0.708878	19	–0.17
2X-2, 140–150	11.4	63.7	0.708560	18	0.33
146-892A-					
2X-3, 0–11	12.6	75.4	0.708411	20	–0.04
3X-2, 0–10	20.6	164.3	0.707718	18	–0.11
4X-2, 0–10	30.1	169.0	0.707589	18	–0.11
6X-2, 0–10	40.6	192.4	0.707461	16	–0.26
146-892D-					
6X-4, 140–150	52.4	211.1	0.707461	20	
146-892A-					
7X-5, 140–150	55.9	208.7	0.707277	18	–0.30
8X-3, 0–10	61.0	229.8	0.707289	21	–0.33
146-892D-					
8X-3, 0–10	64.7	239.1	0.707268	18	–0.49
146-892A-					
9X-1, 69–74	68.2	232.7	0.707168	18	–0.32
146-892D-					
9X-4, 0–15	73.8	250.8	0.707137	17	–0.31
146-892A-					
11X-2, 0–10	79.6	267.2	0.707116	20	–0.48
13X-4, 0–25	101.6	259.4	0.707095	18	–0.52
15X-1, 88–100	116.9	223.7	0.707094	16	
146-892D-					
12X-3, 130–150	123.4	260.2	0.707043	22	
146-892A-					
16X-1, 34–43	125.8	260.2	0.707115	18	–0.61
146-892D-					
13X-CC, 22–24	128.5	272.9	0.707076	15	–0.56
146-892A-					
17X-2, 3–13	136.6	207.5	0.707098	18	–0.68
146-892D-					
14X-1, 115–130	139.2	267.2			–0.67
146-892A-					
18X-1, 115–140	145.8	264.9	0.707126	15	–0.15
146-892D-					
15X-2, 135–150	148.9	267.2	0.707088	21	–0.72
16X-3, 135–150	161.4	267.2			–0.75
16X-5, 135–150	164.4	267.2	0.707069	18	
146-892A-					
20X-2, 0–10	165.1	278.9	0.707109	17	–0.82

from mixing with small amounts of other gases, most likely CO_2. Figure 7 shows the direction of shift of the univariant curve of the methane hydrate stability field by the addition of 7% CO_2 and other components.

Improved field calibrations of the temperature at the BSR at the Chile Triple Junction (CTJ) Site 859, indicate that the depth of the BSR is shallower, and that it occurs at ~2°C higher temperature than the calculated temperature at the depth of the base of the pure H_2O–pure CH_4 stability field (Bangs et al. 1993). Remarkably, at both Sites 889 and 892 in the Cascadia Margin, a similar ~2°C disparity between the depth of the seismically defined position of the BSR and the pure H_2O–pure CH_4 hydrate stability field (shown in Figure 7) was recorded. At Site 889 the BSR is at 224 mbsf, and the in-situ temperature is 14.8°C. The calculated base of the pure H_2O–pure CH_4 hydrate stability field, is 260 mbsf, at 16.8°C (at 1320 m water depth, 2.7°C bottom-water temperature, and 54°C/km geothermal gradient). At Site 892 the BSR is at 74 mbsf and the in situ temperature is 8.5°C. The calculated base of the pure H_2O–pure CH_4 hydrate stability field is 112 mbsf, at 10.4°C (at 670 m water depth, 4.7°C bottom water temperature, and 51°C/km geothermal gradient). It is not surprising that the P–T of the BSR at the CTJ and Cascadia Margin sites better fit the base of the seawater-CH_4 than of the pure H_2O–pure CH_4 hydrate stability field, given the higher quality temperature data acquired at these sites. It is, however, important to note that at these two Cascadia margin sites, as well as at the CTJ Site 859, the temperatures at the BSR depths are consistently lower by ~1°C than the maximum temperature derived from the extrapolated seawater-CH_4 hydrate univariant curve at the corresponding pressures. This significant difference could be due to (1) remaining problems with field calibrations of the temperature at the BSR, which are difficult to obtain; (2) overestimations of the in situ pressures, which is not too likely; (3) the assumption that the maximum temperature of the seawater-CH_4 hydrate stability field remains shifted at a constant ~1.1°C even at pressures >10 MPa; or (4) that the chemistry of the in situ pore fluids, which is different from seawater composition, has an important effect on shifting the maximum temperature of the stability field. Chloride and all major cation concentrations are diluted relative to seawater (Tables 2 and 4). This dilution should have shifted the stability field in the opposite direction (Dickens and Quinby-Hunt, 1994). In addition to the Cl and cation dilutions, the most important chemical differences between seawater and the pore fluids are their notably elevated alkalinities and absence of dissolved sulfate, for example at Site 889 (data in Westbrook, Carson, Musgrave, et al., 1994). The effects of the concentrations of these anions on the stability field of methane hydrate are unknown. Depending on pressures, mixing with other gases, such as CO_2 or H_2S, would also shift the stability field in the opposite direction.

H_2S–CH_4 HYDRATE

Irregularly disseminated gas hydrate crystal aggregates were recovered between ~2 to 19 mbsf in three holes, 892A, 892D, and 892E, at Site 892. This gas hydrate, unlike all others previously recovered, is a mixed hydrate, with both methane and up to 10% H_2S; some ethane (1 to ~600 ppmv) and CO_2 are also present. Adding H_2S to CH_4 decreases the dissociation pressure of the mixed hydrate (e.g., Miller, 1974; Sloan, 1990). The H, C, O, S and Sr-isotope compositions of subsamples from a ~2 cm thick clean CH_4–H_2S hydrate layer, from ~18 mbsf (Kastner and Elderfield, this volume), together with the observation that this hydrate occurs only at 2 to 19 mbsf interval, indicate (1) that the pore fluids within this zone differ from those below it because of mixing with an external to the site fluid source; and (2) that this hydrate system is geologically young (Kastner et al., unpubl. data).

CONCLUSIONS

Inferred from geochemical and geophysical evidence, predominantly methane hydrate exists above the BSRs at both Sites 889 and 892 in the Cascadia margin; Site 889 is characterized by dispersive fluid flow, whereas Site 892 is characterized by confined-fluid flow. At Site 889 disseminated gas hydrate occupies a minimum of 15% of the pore space. A paleo-gas–hydrate zone, at least 70–90 m thick, apparently exists below the BSR. At Site 892 the gas hydrate occupies ≤10% of the pore space of specific sediment horizons. Thus, the high amplitudes of these BSRs are not simply related to gas hydrate content but to the interplay between its content and the presence and concentration of free gas below the BSR. The estimated P–T of these BSRs better fit the base of the extrapolated seawater-methane hydrate stability field than that of the pure H_2O–pure CH_4 one. However, the estimated temperatures at the BSRs at both sites are lower by almost 1°C than the predicted maximum temperatures from the seawater-CH_4 base of the stability field at the appropriate depths (pressures). This disparity is caused by either uncertainties in the temperature and BSR depth estimates, or, if real, by the chemical composition of minor constituents (not just salinity) of the pore fluids, which differs considerably from that of seawater.

The strongest geochemical and geological evidence for the presence of primarily methane hydrate after dissociation caused by drill-

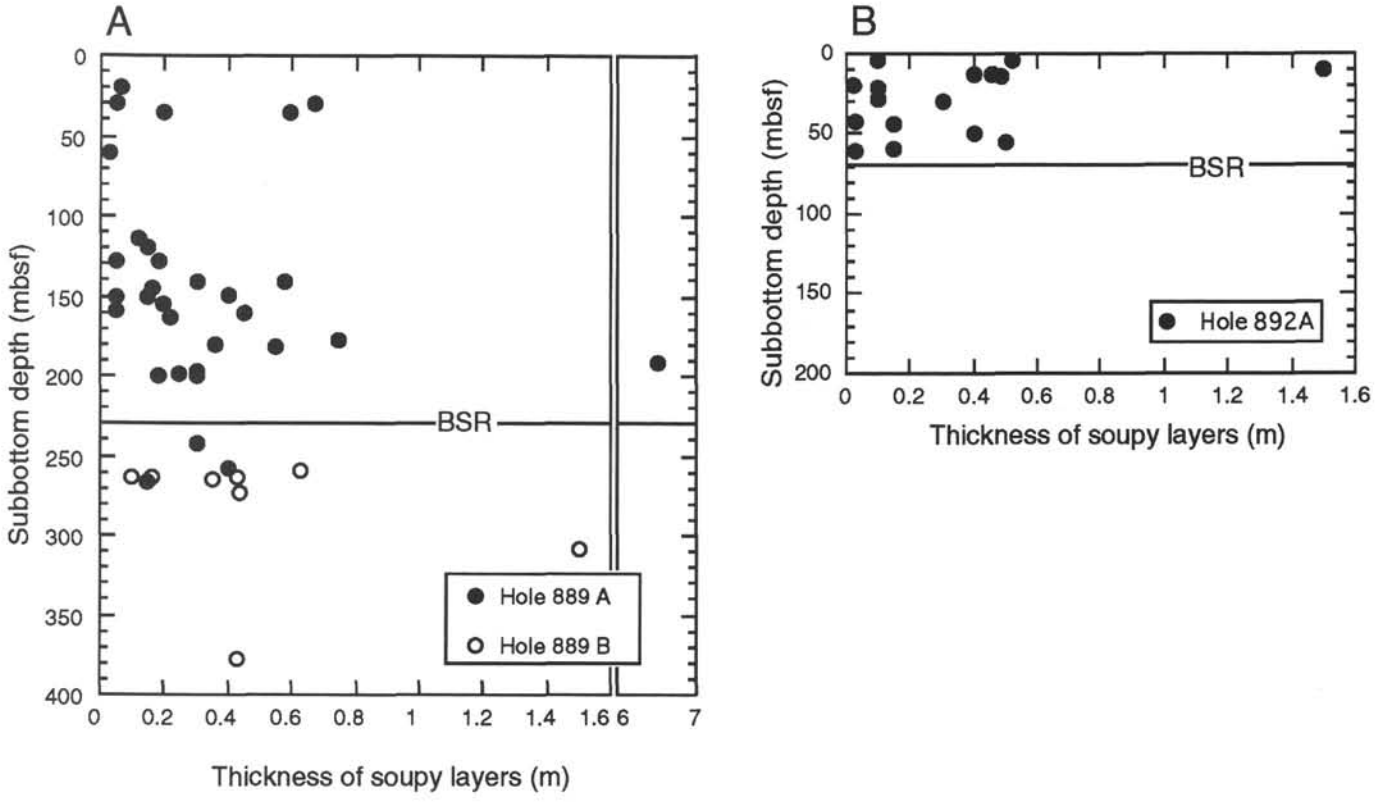

Figure 6. Depth distribution of "soupy" sediment intervals at **(A)** Site 889 and **(B)** Site 892.

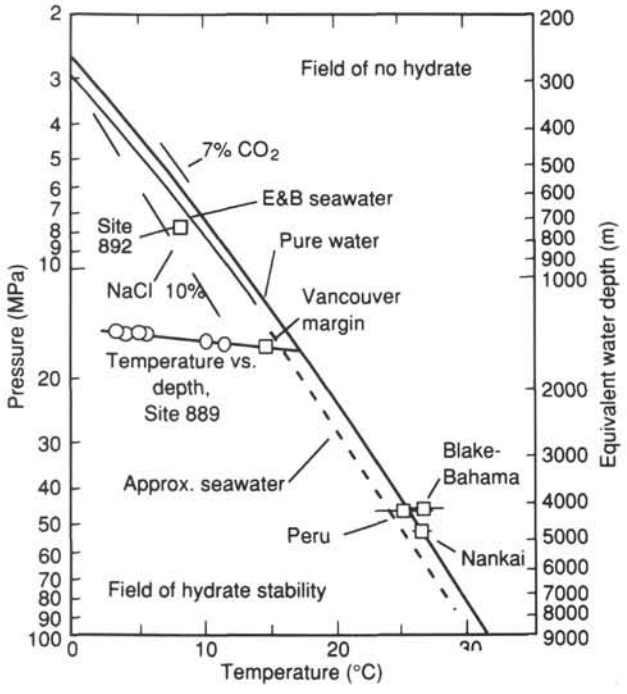

Figure 7. The stability fields of methane hydrate from compilation of Sloan (1990). The seawater dashed curve is from the equation of state derivation for artificial seawater by Englezos and Bishnoi (1988) (= E&B) and from the experimental seawater–CH_4 hydrate data by Dickens and Quinby-Hunt (1994).

ing and coring operations consists of the following observations: lower than in situ Cl concentration, dilution of the other major seawater cations equivalent to Cl, high methane concentration, lower than bottom water core temperature, "soupy" sediment interval, and enhanced seismic velocity.

A fluid rich in CH_4 and containing ethane, advecting from intermediate depth into the in situ sulfate reducing zone and migrating along a low-angle fault, is responsible for the formation of the mixed CH_4–H_2S hydrate near the sediment/seawater interface at 2–19 mbsf.

ACKNOWLEDGMENTS

We greatly appreciate the Leg 146 shipboard scientists for stimulating dialogues, we thank the technicians for their assistance, specifically the ODP chemistry technicians Anne Pimmel and Dennis K. Graham for their skillful help in the shipboard geochemical work, and the staff and drilling crews aboard the *JOIDES Resolution* for their cooperation. We are especially grateful for Dr. G. Lugmair at Scripps Institution of Oceanography for his assistance in the Sr isotopic analyses. The manuscript greatly benefitted from reviews by Drs. R.D. Hyndman, R.C. Burruss, and M. Rowe. This research was supported by a JOI-USSAC grant and by an NSF grant OCE 91-15784 to M. Kastner.

REFERENCES

Arnason, B., 1969. Equilibrium constant for the fractionation of deuterium between ice and water. *J. Phys. Chem.*, 73:3491–3494.

Bangs, N.L.B., Sawyer, D.S., and Golovchenko, X., 1993. Free gas at the base of the gas hydrate zone in the vicinity of the Chile triple junction. *Geology*, 21:905–908.

Carson, B., Seke, E., Paskevich, V., and Holmes, M.L., 1994. Fluid expulsion sites on the Cascadia accretionary prism: mapping diagenetic deposits with processed GLORIA imagery. *J. Geophys. Res.*, 99:11959–11969.

Carson, B., Suess, E., and Strasser, J.C., 1990. Fluid flow and mass flux determinations at vent sites on the Cascadia margin accretionary prism. *J. Geophys. Res.*, 95:8891–8897.

Craig, H., and Hom, B., 1968. Relationship between deuterium, oxygen-18 and chlorinity in the formation of sea ice. *Trans. Am. Geophys. Union,* 49:216–217.

Davidson, D.W., El-Defrawy, M.K., Fuglem, M.O., and Judge, A.S., 1978. Natural gas hydrates in northern Canada. *Proc. 3rd Int. Conf. Permafrost,* 3:937–943.

Davidson, D.W., Leaist, D.G., and Hesse R., 1983. Oxygen-18 enrichment in water of a clathrate hydrate. *Geochim. Cosmochim. Acta.,* 47:2293–2295.

Dholabhai, P.D., Englezos, P., Kalogerakis, N., and Bishnoi, P.R., 1991. Equilibrium conditions for methane hydrate formation in aqueous mixed electrolyte solutions. *Can. J. Chem. Eng.,* 69:800–805.

Dickens, G.R., and Quinby-Hunt, M.S., 1994. Methane hydrate stability in seawater. *Geophys. Res. Lett.,* 21:2115–2118.

Englezos, P., and Bishnoi, P.R., 1988. Predictions of gas hydrate formation conditions in aqueous solutions. *Am. Inst. Chem. Eng.,* 34:1718–1721.

Hesse, R., Lebel, J., and Gieskes, J.M., 1985. Interstitial water chemistry of gas-hydrate-bearing sections on the Middle America Trench slope, Deep-Sea Drilling Project Leg 84. *In* von Huene, R., Aubouin, J., et al., *Init. Repts. DSDP,* 84: Washington, DC (U.S. Govt. Printing Office), 727–737.

Hyndman, R.D., and Davis, E.E., 1992. A mechanism for the formation of methane hydrate and seafloor bottom-simulating reflectors by vertical fluid expulsion. *J. Geophys. Res.,* 97:7025–7041.

Hyndman, R.D., Foucher, J.P., Yamano, M., Fisher, A., Berner, U., et al., 1992. Deep sea bottom-simulating-reflectors: calibration of the base of the hydrate stability field as used for heat flow estimates. *Earth Planet. Sci. Lett.,* 109:289–310.

Hyndman, R.D., and Spence, G.D., 1992. A seismic study of methane hydrate marine bottom simulating reflectors. *J. Geophys. Res.,* 97:6683–6698.

Hyndman, R.D., Wang, K., Yuan, T., and Spence, G.D., 1993. Tectonic sediment thickening, fluid expulsion, and the thermal regime of subduction zone accretionary prisms: the Cascadia margin off Vancouver Island. *J. Geophys. Res.,* 98:21865–21876.

Kastner, M., Elderfield, H., and Martin, J.B., 1991. Fluids in convergent margins: what do we know about their composition, origin, role in diagenesis and importance for oceanic chemical fluxes? *Philos. Trans. R. Soc. London A,* 335:243–259.

Katz, D.L., Cornell, D., Kobayashi, R., Poettmann, F.H., Vary, J.A., Elenbaas, J.R., and Weinaug, C.F., 1959. Water-hydrocarbon systems. *In* Katz, D.L., et al. (Eds.), *Handbook of Natural Gas Engineering:* New York (McGraw-Hill), 189–221.

Kulm, L.D., Suess, E., Moore, J.C., Carson, B., Lewis, B.T., Ritger, S.D., Kadko, D.C., Thornburg, T.M., Embley, R.W., Rugh, W.D., Massoth, G.J., Langseth, M.G., Cochrane, G.R., and Scamman, R.L., 1986. Oregon subduction zone: venting, fauna, and carbonates. *Science,* 231:561–566.

Kvenvolden, K.A., 1988. Methane hydrate—a major reservoir of carbon in the shallow geosphere? *Chem. Geol.,* 71:41–51.

Kvenvolden, K.A., and Kastner, M., 1990. Gas hydrates of the Peruvian outer continental margin. *In* Suess, E., von Huene, R., et al., *Proc. ODP, Sci. Results,* 112: College Station, TX (Ocean Drilling Program), 517–526.

Kvenvolden, K.A., and McMenamin, M.A., 1980. Hydrates of natural gas: a review of their geologic occurrence. *Geol. Surv. Circ. (U.S.),* 825.

Lawrence, J.R., Gieskes, J.M., and Broecker, W.S., 1975. Oxygen isotope and cation composition of DSDP pore waters and the alteration of Layer II basalts. *Earth Planet. Sci. Lett.,* 27:1–10.

MacKay, M.E., Jarrard, R.D., Westbrook, G.K., and Hyndman, R.D., 1994. Origin of bottom-simulating reflectors: geophysical evidence from the Cascadia accretionary prism. *Geology,* 22:459–462.

Makogon, Y.F., 1981. *Hydrates of Natural Gas:* Tulsa, OK (PennWell). (Trans. by W.J. Cieslesicz)

Menton, P.D., Parrish, W.R., and Sloan, E.D., 1981. Effect of inhibitors on hydrate formation. *Ind. Eng. Chem. Process Des. Dev.,* 20:399–401.

Merlivat, L., and Nief, G., 1967. Fractionnement isotopique lors de changement d'état solide-vapeur et liquide-vapeur de l'éau a des températures à 0°C. *Tellus,* 19:122–127.

Miller, S.L., 1974. The nature and occurrence of clathrate hydrates. *In* Kaplan, I.R. (Ed.), *Natural Gases in Marine Sediments:* New York (Plenum), 151–177.

Mitchell, C.E., Vincent, P., Weldon, R.J., and Richards, M.A., 1994. Present-day vertical deformation of the Cascadian margin, Pacific Northwest, United States. *J. Geophys. Res.,* 99:12257–12277.

Moore, J.C., Orange, D., and Kulm, L.D., 1990. Interrelationship of fluid venting and structural evolution: *Alvin* observations from the frontal accretionary prism. *J. Geophys. Res.,* 95:8795–8808.

O'Neil, J.R., 1968. Hydrogen and oxygen isotope fractionation between ice and water. *J. Phys. Chem.,* 72:3683–3684.

Platteeuw, J.C., and van der Waals, J.H., 1958. Thermodynamic properties of gas hydrates. *Mol. Phys.,* 1:91–96.

Perry, E.A., and Hower, J., 1972. Late-stage dehydration in deeply buried pelitic sediments. *AAPG Bull.,* 56:2013–2021.

Ransom, B., Spivack, A.J., and Kastner, M., 1995. Stable chlorine isotopes in subduction zone pore waters: implications for fluid-rock reactions and the cycling of chlorine. *Geology,* 23:715–718.

Serra, O., 1984. *Fundamentals of Well-Log Interpretation* (Vol. 1): *The Acquisition of Logging Data:* Amsterdam (Elsevier).

Sloan, E.D., 1990. *Clathrate Hydrates of Natural Gasses:* New York (Marcel Dekker).

Suzuki, T., and Kimura, T., 1973. D/H and $^{18}O/^{16}O$ fractionation in ice-water systems. *Mass Spectros. (Tokyo),* 21:229–233.

van der Waals, J.H., and Platteeuw, J.C., 1959. Clathrate solution. *Adv. Chem. Phys.,* 2:1–57.

Wang, K., Hyndman, R.D., and Davis, E.E., 1993. Thermal effects of sediment thickening and fluid expulsion in accretionary prisms: model and parameter analysis. *J. Geophys. Res.,* 98:9975–9984.

Westbrook, G.K., Carson, B., Musgrave, R.J., et al., 1994. *Proc. ODP, Init. Repts.,* 146 (Pt. 1): College Station, TX (Ocean Drilling Program).

Yamamoto, S., Alcauskas, J.B., and Crozier, T.E., 1976. Solubility of methane in distilled and seawater. *J. Chem. Eng. Data,* 21:78–80.

Date of initial receipt: 9 December 1994
Date of acceptance: 31 May 1995
Ms 146SR-213